A Comprehensive Investigation of Injection-Induced Earthquakes in Northeastern British Columbia, Canada

Geoscience BC Report 2022-10

Results of Research

Geoscience BC Research Project 2019-007

Dr. Honn Kao

School of Earth and Ocean Sciences, University of Victoria, Victoria, BC
Geological Survey of Canada, Natural Resources Canada, Sidney, BC

Geoscience BC

Natural Resources Canada   Ressources naturelles Canada

University of Victoria

A Comprehensive Investigation of Injection-Induced Earthquakes in Northeastern British Columbia, Canada

Dr. Honn Kao

School of Earth and Ocean Sciences, University of Victoria, Victoria, BC
Geological Survey of Canada, Natural Resources Canada, Sidney, BC

Table of Contents

Executive Summary

Vast amounts of Canada's hydrocarbon resources are locked inside unconventional reservoirs. Economic development of unconventional hydrocarbons depends on effective hydraulic fracturing (HF) treatments and wastewater disposal (WD) into deep saline aquifers. Both HF and WD have been linked to induced earthquakes with seismic hazard implications.

Previous research suggested that HF operations were responsible for most felt injection-induced earthquakes (IIE) in western Canada. A recent study conducted by Natural Resources Canada (NRCan) suggests that IIE tend to cluster in specific areas with different occurrence rates and/or magnitude ranges. It is unclear how such variation is controlled by injections, site-specific geomechanical conditions, local and/or regional geological/tectonic setting, or a combination of some of the factors.

In this project, we conduct a comprehensive investigation of IIE in British Columbia's Northeast Region. Our research activities are grouped into four work plans. They are:

WP1: Efficient Management of the McGill Array and Data Sharing

WP2: Establishing the Most Comprehensive and Accurate IIE Catalogues

WP3: Delineating Source Characteristics of Significant IIE in Northeast BC

WP4: Delineation of Significant Factors Controlling the Seismogenesis of IIE

To ensure the best seismic observation available, we continue operating a dense array established by McGill University in the Fort St. John–Dawson Creek area (WP1). As we take over the McGill Array operation, we make all the real-time data freely available to all users (WP1). Based on the improved seismic data and newly developed methods, we established the most comprehensive and accurate earthquake catalogues for northeast BC. These catalogues are made available to the public as two Geological Survey of Canada (GSC) Open File reports (WP2, Appendix A and Appendix B).

With the enhanced earthquake catalogues, we investigated the source characteristics of significant IIE in northeast BC and their relationship to injection parameters at nearby wells (WP3). A series of seven papers focusing on different topics and events were published as the results of this research effort (Appendices C–I).

Finally, we delineated significant factors that influence the seismogenic pattern of IIE in northeast BC (WP4). We took a machine-learning-based approach to differentiate the relative importance of all the physical parameters, including both geological and operational, in controlling the local seismic pattern. Three papers on this topic have been published. These are provided as Appendix J, K and L (pre-print).

Our research results provide high-resolution IIE monitoring for northeast BC and fill clear knowledge gaps in understanding the seismogenic conditions of IIE. The improved earthquake catalogues and physical models are useful to regulators to achieve a strategic balance between the economic prosperity from unconventional hydrocarbon development and the protection of public safety and the environment. Our project outputs also help the oil & gas industry by providing fundamental knowledge on IIE to better understand the seismic hazards and effectively mitigate the negative impact of HF and/or WD associated with the development of unconventional hydrocarbon resources. Local communities also benefit from this project through more accurate assessment of seismic hazard from IIE.

Background and Previous Works

Oil and gas production is one of the pillars of the Canadian economy, accounting for almost 10% of its national GDP. The Western Canada Sedimentary Basin (WCSB) is well known for its subsurface hydrocarbon resources associated with thick sedimentary formations [1]. Consequently, sustained development of the hydrocarbon resources has been, and still is, a vital part of BC's economic growth.

Vast amounts of Canada's hydrocarbon resources are locked inside shale and siltstone formations (also known as unconventional reservoirs). A common practice in the industry to maximize the efficiency of gas extraction from these formations is horizontal drilling accompanied by intensive hydraulic fracturing (HF) treatments. Another common practice of injection is to dispose of flow-back HF fluids and industrial wastewater into deep saline aquifers (i.e., wastewater disposal, WD). The BC Oil and Gas Commission (BCOGC) reported that approximately 87% of gas production in BC is from unconventional sources [2].

It has been demonstrated that high-pressure fluid injection may elevate the level of background seismicity and sometimes induce significant (felt) earthquakes both in Canada [3-6] and abroad [7-10]. In western Canada specifically, the distribution of regional seismicity has closely followed unconventional gas development activities from the Horn River Basin in 2006-2011 to the Montney Play since 2013. To properly study the occurrence of IIE and their seismogenic characteristics, multiple efforts have been made to densify the seismograph networks in major unconventional gas basins since 2013 [11]. These efforts led to significantly improved monitoring capability for IIE, and contributed to a series of regulatory changes aiming at mitigating the seismic hazard associated with the unconventional hydrocarbon development [12].

In BC, the two largest IIE (M_w 4.6 on 17 August 2015 and M_w 4.5 on 30 November 2018) were both associated with HF within the Montney Play [6,13]. The uniquely shallow depths of such events caused significant ground shaking (with Peak Ground Acceleration as high as 17% g at a distance of ~5 km from the epicenter), despite the relatively small magnitudes [14]. Most of the significant/felt IIE in BC appeared to occur within the sedimentary layer above the crystalline basement [6,15], as opposed to observations in central United States where the majority of significant IIE were associated with faults within the basement [16]. A detailed earthquake relocation study by NRCan seems to suggest that IIE tend to cluster in specific areas with different occurrence rates and/or magnitude ranges. It is unclear how such variation of seismogenic behavior is controlled by injections, site-specific geomechanical conditions, local and/or regional geological/tectonic setting, or a combination of some or all of them.

An important source of seismic data for studying the IIE in northeast BC is the dense seismic array established by McGill University since 2015, which was supported by an NSERC Strategic Project grant. The purpose of this array deployment was to provide near-field observations to constrain source models that can be used for the assessment and mitigation of seismic hazards associated with the unconventional hydrocarbon development. The McGill Array has eight broadband stations and was originally deployed in northern Montney near the epicenter of the 17 August 2015, M_w 4.6, earthquake. As HF ramped up in the Fort St. John–Dawson Creek area, the array was relocated southward to cover sectors with the highest number of injection wells. At the same time, the array was upgraded to real-time data transmission to complement the sparse coverage of the regional network in southern Montney. The McGill Array's contribution to real-time IIE monitoring is remarkable, as reflected by the large number of events detected in the Fort St. John–Dawson Creek area [17]. In fact, the McGill stations have consistently been the most used in locating regional and local earthquakes in western Canada. Data from individual McGill stations were also integrated by local operators into their own real-time IIE monitoring (Fig. 1).

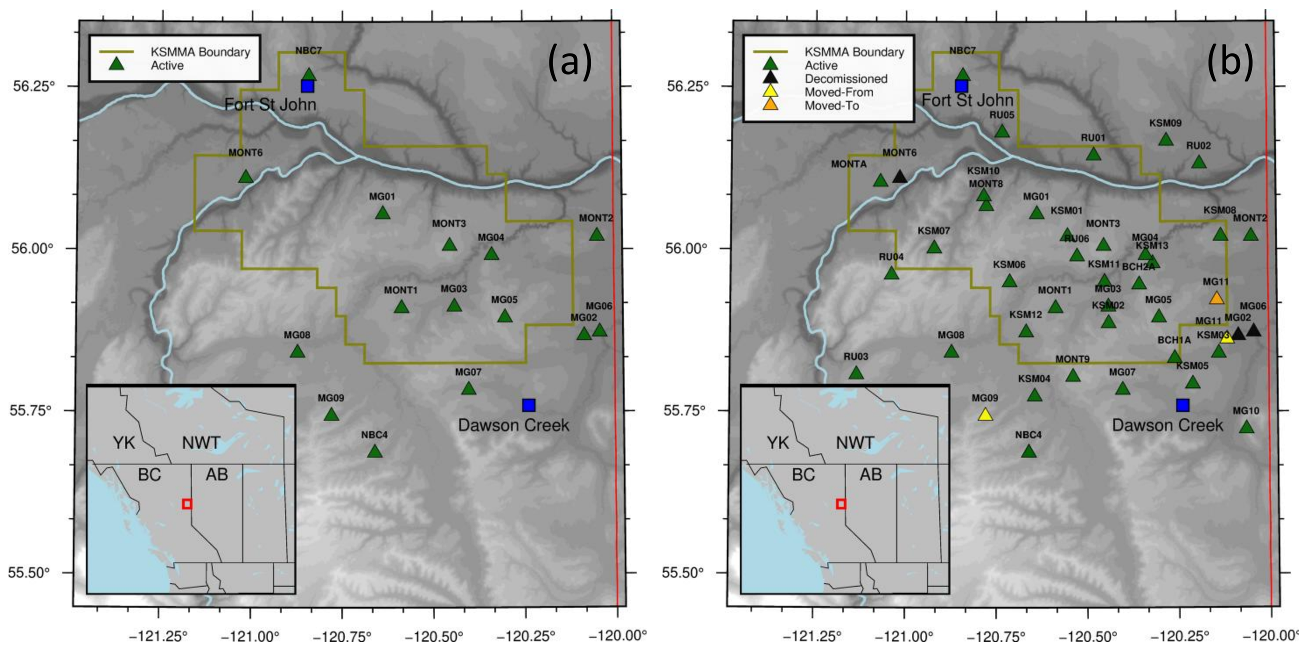

Figure 1. Location of seismic stations in the years of 2018 and 2022. (a) Green triangles show the location of active seismic stations in 2018. McGill stations are those operated by this project. The brown line marks the outline of the KSMMA. (b) Active (green), decommissioned (black), and newly installed (orange) seismic stations in the KSMMA by the end of 2021. Notice that MG09 was moved out of the map boundary (not shown).

Unfortunately, funding to McGill University for the McGill Array was terminated in 2020. It was deemed extremely important to continue operating the array for at least three reasons. First, both HF and WD operations in the area are expected to continue in the foreseeable future, making it the most likely place for IIE to occur. Secondly, BCOGC needs precisely determined earthquake locations and depths to make effective regulatory decisions. Without McGill stations, earthquake source parameters can have larger uncertainties that may lead to unnecessary confusion by the general public and/or economic consequences to local operators. And thirdly, the McGill Array had been in operation in the area for only two years at the time when this current Geoscience BC research project was proposed (2017-2019). The dataset is insufficient for time-dependent regional/local seismic hazard analysis, which is considered more appropriate for the case of IIE [18].

As part of this Geoscience BC project, which commenced November, 2019, we successfully continue the routine operation of the McGill Array with a new open-data policy to make its real-time data freely available to all users. Meanwhile, we take advantage of the wealth of the much-improved seismic observations in western Canada, including the McGill Array, to conduct a comprehensive investigation into the seismogenic conditions of IIE in northeast BC. Specifically, this project consists of four work plans:

WP1: Efficient Management of the McGill Array and Data Sharing

WP2: Establishing the Most Comprehensive and Accurate IIE Catalogues

WP3: Delineating Source Characteristics of Significant IIE in Northeast BC

WP4: Delineation of Significant Factors Controlling the Seismogenesis of IIE

These work plans are designed to align with the recommendations by the Scientific Hydraulic Fracturing Review Panel in their recently published report [19]. The outputs of our research not only help regulators develop the best strategy for a balanced approach between economic benefit and the protection of public safety and the environment, but also benefit the oil and gas industry by providing fundamental knowledge on IIE to effectively mitigate the seismic hazard associated with the development of unconventional hydrocarbon resources. The scientific and economic merits are in perfect accord with Geoscience BC's vision of "being a leading partner and provider of credible and relevant earth science research and data in British Columbia."

In the following sections, we systematically describe the major accomplishments under each work plan. Most of the research results have been published in peer-reviewed international journals. Reprints of the published papers and reports are included as separate Appendices along with the publication of this report.

WP1: Efficient Management of the McGill Array and Data Sharing

Our first task was to ensure the continuing operation of the McGill Array (FDSN network code XL). We not only took over the responsibility of the McGill Array, but also worked closely with our partners, including NRCan, BCOGC, and Ruhr University Bochum (RUB), to coordinate maintenance services to seismograph stations in the Montney area (FDSN network codes 1E and PQ). The stable operation of the McGill Array and other seismograph stations in northeast BC has helped regulators gain real-time information on injection-related seismicity in the most productive area of unconventional gas and tight oil in BC. The operational periods for seismic stations in the KSMMA are shown in Fig. 2.

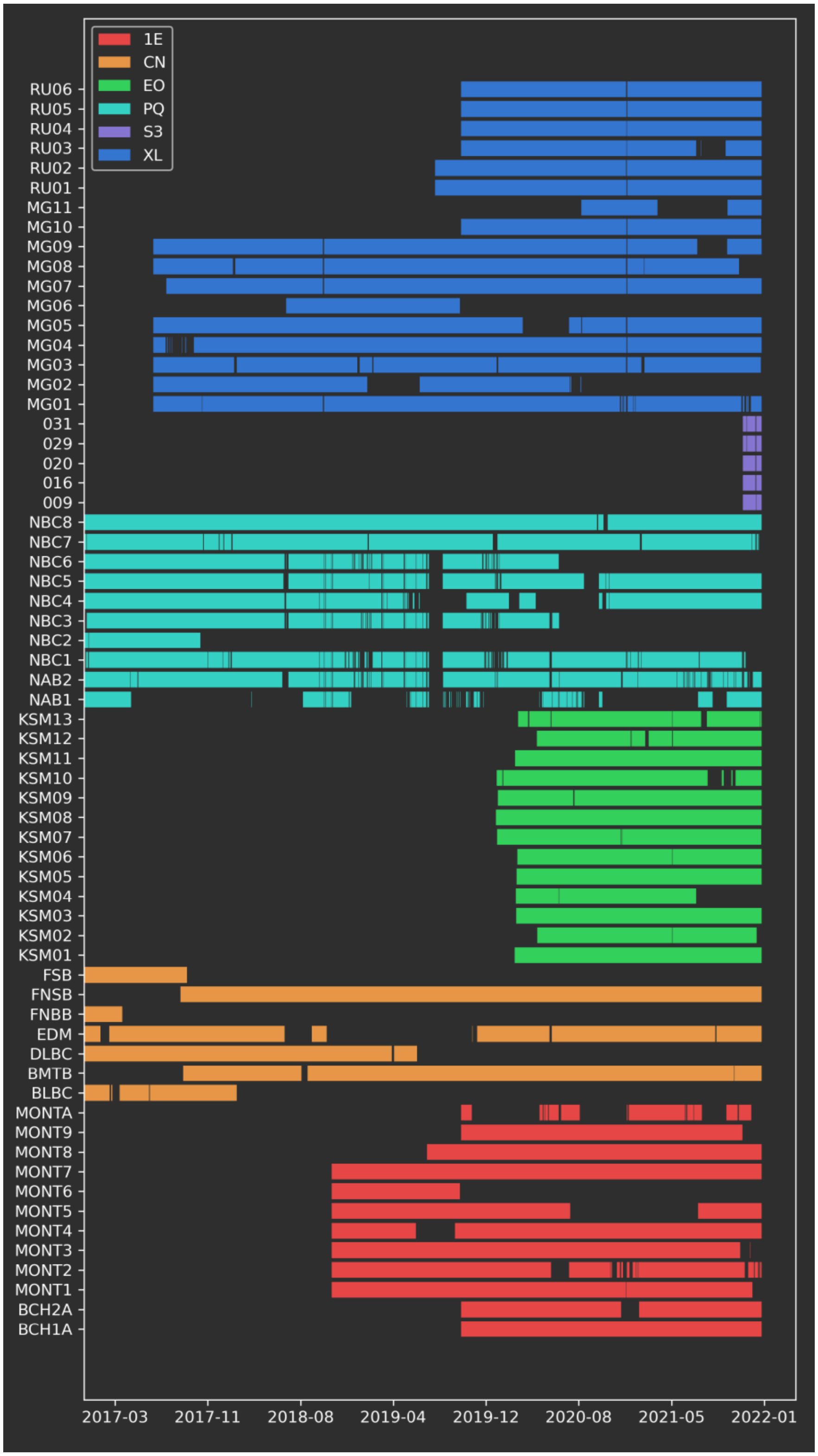

Figure 2. Operational periods for multiple networks in the KSMMA. Seismic stations marked with same colour correspond to the same network. The XL network with eleven seismic stations is maintained by this project.

Under this work plan, two field trips were conducted to provide necessary maintenance and service. Details of the two trips are summarized below:

1. The first service trip was conducted at the McGill Array to fix a number of instrument issues. Due to the COVID-19 travel restrictions, we had to hire a team of two field technicians from Nanometrics Inc. to complete the service trip in early July (from July 9 to 14, 2021). The following works were completed (see Fig. 1 for station locations):
    a. Station MG09 was removed as requested by the landowner
    b. Station MG07's faulty digitizer was replaced
    c. Station MG11 was removed to avoid flooding
    d. Adjust solar panels at stations BCH1A and BCH2A to improve charging efficiency
    e. Replace the sensor cable at station MG01
    f. Replace batteries for station NAB1
    g. Restart the seismic sensor at station MONT5

2. The second field trip was conducted to visit seismograph stations in the Fort St. John–Dawson Creek area, including the McGill Array and those operated by RUB and NRCan, to fix a number of instrument issues. The service trip was completed in late September to early October 2021. Two teams were assembled to make the fieldwork more efficient (Team 1: Dr. Ramin Dokht and Dr. Ali Babaie Mahani, Team 2: Dr. Bei Wang and Mr. Greg Langston). The following works were completed, along with photos taken at the scene.

    a. Stations RU01, RU02, RU06, MG08, and MONT3 were visited and cleaned to ensure normal operation (see Fig. 1 for station locations)

b. Stations MG03 and MG05 were visited and inspected to ensure normal operation (see Fig. 1 for station locations)

c. Stations MONT9, RU03 and RU04 were visited and adjusted to ensure normal operation (see Fig. 1 for station locations)

d. Station NAB1 had a power failure. It was fixed with a replacement of one of its solar panels (see Fig. 1 for station location)

e. Stations MG10 and MONT2 were visited and inspected. No issues were found (see Fig. 1 for station locations, no photo for this visit)

f. Replace SIM cards for stations RU03, MONTA, and MG08 (see Fig. 1 for station locations)

g. Relocate stations MG09 and MG11 to new sites (see Fig. 1 for station locations)

h. Convert NBC4 from VSAT communication to a cell modem (see Figure 1 for station location, no photo for this visit)

Overall, the McGill Array and other seismograph stations operated by our partners play a vital role in the effective monitoring of injection-induced earthquakes in northeast BC. All seismograph stations are transmitting data directly to the Apollo server in NRCan's Geological Survey of Canada, Sidney office (Pacific Geoscience Centre) for real-time processing. Another data stream goes to the Data Management Center of the Incorporated Research Institution for Seismology (IRIS) for public distribution. This open-data policy allows direct data access to individual stations that can enhance local operators' real-time earthquake monitoring during HF treatments.

There is a strong consensus among BCOGC, NRCan, McGill University, and the energy industry to continue the operation of these stations after this Geoscience BC project is ended. The detailed technical plan remains to be worked out.

WP2: Establishing the Most Comprehensive and Accurate IIE Catalogues

This work plan aimed at establishing the most comprehensive and accurate earthquake catalogues for northeast BC, taking advantage of the increasing number of seismograph stations in the region and newly developed earthquake location methods. Overall, we were able to detect and locate 23753 earthquakes within the KSMMA during 2019–2021, with a magnitude of completeness of ~0.8 (Fig. 3).

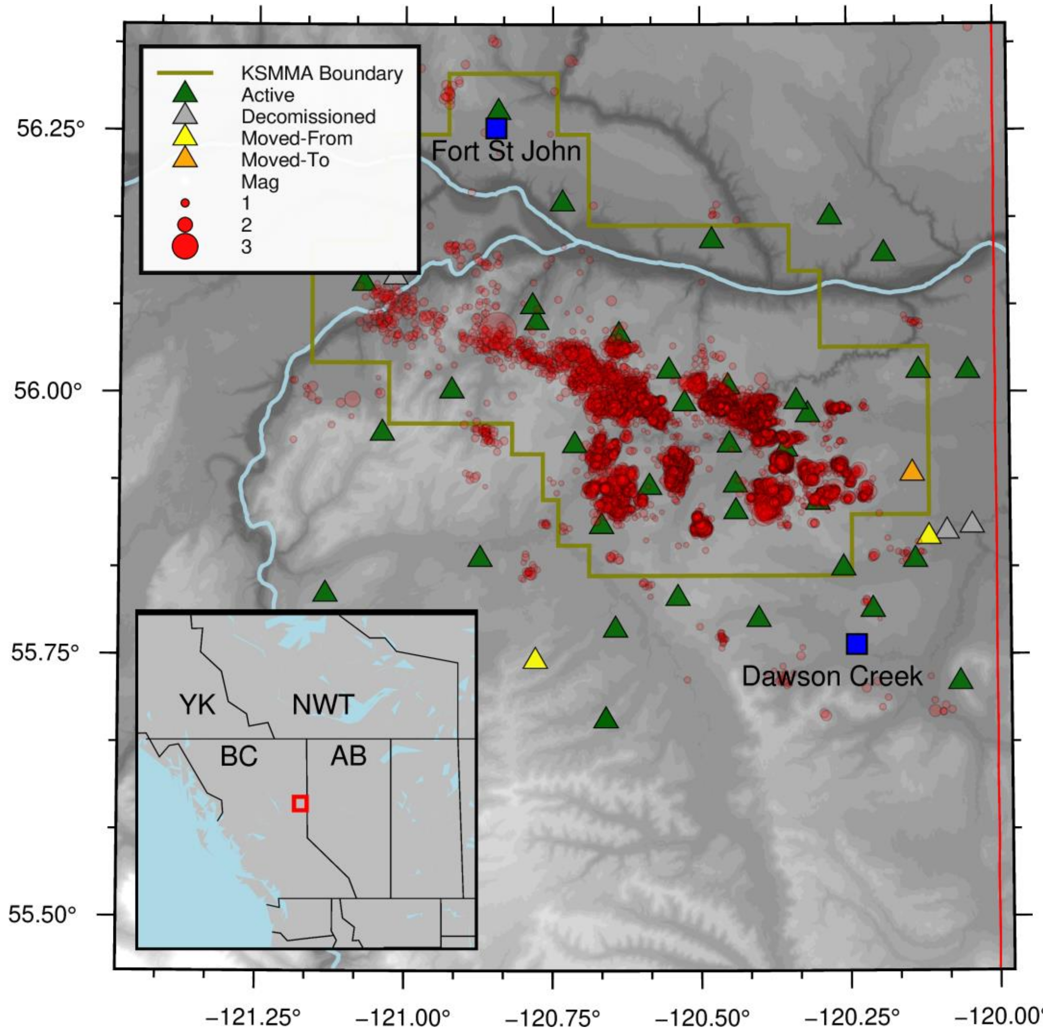

Figure 3. Seismicity from the enhanced catalogue for the KSMMA during 2019–2021. Red circles represent the detected and located earthquakes, and the symbol size corresponds to the event magnitude. Inset shows the geographic location of the KSMMA. Other layouts are the same as Figure 1.

We published our IIE catalogues as Geological Survey of Canada (GSC) Open File reports with complete technical details. The catalogue for 2021 is expected to be published in late 2022 or early 2023 depending on the GSC's internal review timing. We also developed an artificial intelligence (AI)-based earthquake location system that is capable of real-time monitoring of IIE without human intervention. The publication details of these products are summarized below.

1. Visser, R., H. Kao, B. Smith, C. Goerzen, B. Kontou, R.M.H. Dokht, J. Hutchinson, F. Tan, and A. Babaie Mahani (2020). A comprehensive earthquake catalogue for the Fort St. John–Dawson Creek region, British Columbia, 2017–2018, Geological Survey of Canada Open File 8718, one .zip file, https://doi.org/10.4095/326015.

   This catalogue contains earthquakes that were detected and located using a combination of manual analysis and a semi-automated process utilizing the newly developed Seismicity-Scanning based on the Navigated Automatic Phase-picking (S-SNAP) algorithm. A reprint of this publication is included in Appendix A.

2. Visser, V., H. Kao, R.M.H. Dokht, A. Babaie Mahani, and S. Venables (2021). A comprehensive earthquake catalogue for Northeastern British Columbia: The Northern Montney Trend from 2017 to 2020 and the Kiskatinaw Seismic Monitoring and Mitigation Area from 2019 to 2020, Geological Survey of Canada Open File 8831, one .zip file, https://doi.org/10.4095/329078.

   In this study, we deploy two different machine-learning models to identify earthquake phases using waveform data from regional seismic stations and utilize an earthquake database management system to streamline the construction and maintenance of an up-to-date earthquake catalogue. The completion of this study allows for a comprehensive catalogue in northeast BC from 2014 to 2020 by building upon our previous 2014–2016 and 2017–2018 catalogues. A reprint of this publication is included in Appendix B.

WP3: Delineating Source Characteristics of Significant IIE in Northeast BC

In the third workplan, we investigated the source characteristics of significant IIE in northeast BC and their relationship to injection parameters at nearby wells. This work plan was designed to delineate source characteristics of significant IIE in northeast BC that, in turn, contribute to better understanding of the corresponding seismogenic conditions.

We found that the stress drop of the largest IIE (M_w 4.6) in the WCSB is well within the range of tectonic events (Fig. 4), suggesting that the M_w 4.6 sequence likely occurred on a pre-existing fault. We also investigated the triggering mechanisms of this sequence, and we found that pore pressure increase associated with the migration of injected fluid is required to accumulate sufficient stress perturbations to trigger the M_w 4.6 earthquake.

With a comprehensive analysis of the intensity distribution associated with IIE in northeast BC, we determine that the ground shaking intensity from shallow IIE events (depth <5 km) can be higher than those at deeper depths (>10 km) at close distances (10–15 km). But the intensity tends to decrease rapidly at greater distances and become lower than that caused by deep events.

While investigating the spatiotemporal distribution of IIE, we found that the cross-correlation coefficient (CC) is not a reliable proxy for the identification of repeating earthquakes. For reliable repeater identification, a better alternative is to require the inter-event distance to be smaller than the rupture area of the larger event.

We report a new type of IIE, named "earthquakes characterized by hybrid-frequency waveforms" (EHW), that are characterized by broader P- and S-pulses and relatively lower frequency content in the coda wave train (Fig. 5). Detailed source analysis indicates that EHW have generally lower stress drop, slower rupture speed, or a combination of both. The slower rupture speed and/or lower stress drop values of EHW probably represent the manifestation of slow rupture transitioning from aseismic to seismic slip.

Finally, we re-examined the 2015 IIE sequence in the Fox Creek area, Alberta, with high-resolution earthquake relocation methods. Our results reveal a complex first-outward-then-inward IIE migration pattern. This 3D pattern can successfully explain the observed delayed triggering and required rapid pore-pressure build-up from HF at local distance.

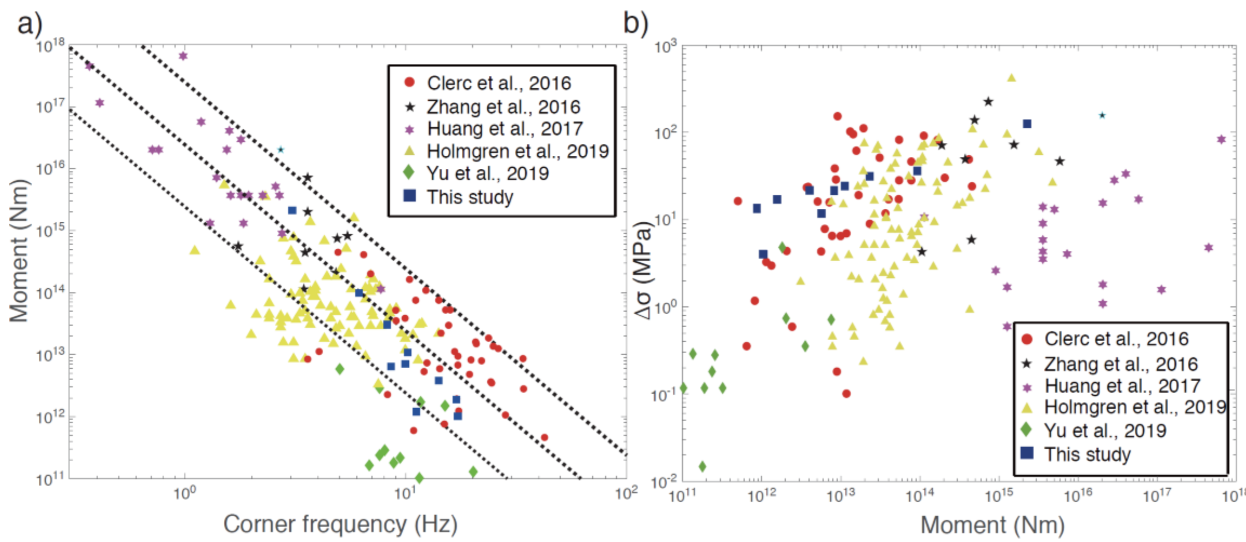

Figure 4. a) Corner frequency vs. seismic moment of the induced seismicity in the WCSB and central United States compiled from different studies. Dashed lines represent lines of constant stress drop assuming a constant shear velocity of 2.8 km/s. b) Stress drop values calculated with the Madariaga model for earthquakes as shown in (a). In both plots, circles denote values for induced earthquakes in Fox Creek, Alberta from Clerc et al. (2016). Black stars denote the values for induced earthquakes in the WCSB from Zhang et al. (2016). Triangles denote induced earthquakes in the WCSB from Holmgen et al. (2019). Diamonds denote the induced earthquakes with moment > 1011 Nm in the Montney Basin from Yu et al. (2019). Hexagons represent the induced earthquakes resulting from wastewater injection in the central United States from Huang et al. (2017). Blue squares denote the stress drop values derived in this study.

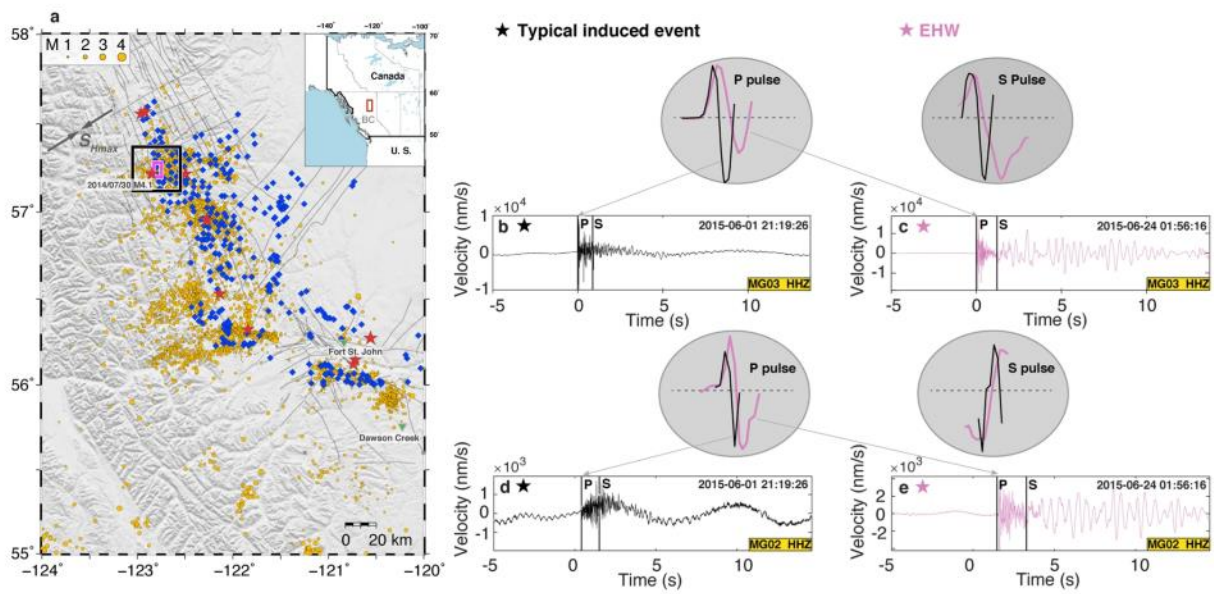

Figure 5. a) Hydraulic fracturing activity and seismicity in northeast BC. The top-right inset shows the geographic location of the study area (red rectangle). Blue diamonds: hydraulic fracturing injection wells between January 1, 2014 and December 31, 2016, reported by the BCOGC. Yellow dots: earthquakes. Stars: 10 M_w 4–5 earthquakes since 2008. Black rectangle: study area in which EHWs occurred. b) and c) Comparison between representative examples of a typical induced event (black trace) and an EHW (purple trace). Both waveforms are from the vertical component of station MG03 with comparable source-station distance (1.32 km vs. 1.65 km) and magnitudes (~M_w 1.5). Manually picked P/S-arrivals are marked. The comparison of P/S-pulse shape demonstrates the relatively wider pulses for EHWs. d) and e) The same as (b) and (c), but for waveforms recorded at station MG02. Both events show longer coda durations with slightly larger epicentral distances. Note that although both types of events have extended coda durations, the EHW contains a relatively larger proportion of lower-frequency energy in the coda.

Key outputs are listed below:

1. Wang, B., R.M. Harrington, Y. Liu, H. Kao, and H. Yu (2020). A study on the largest hydraulic-fracturing-induced earthquake in Canada: Observations and static stress drop estimation, *Bulletin of the Seismological Society of America, 110*, 2283-2294, https://doi.org/10.1785/0120190261.

This study focuses on the source characteristics of the largest hydraulic fracturing-induced earthquake in BC (i.e., the 17 August 2015, M_w 4.6, earthquake northwest of Fort St. John). Stress-drop values estimated using seismic moment and corner frequency from single-event spectra and spectral ratios range from ∼ 1 to 35 MPa, within the typical range of tectonic earthquakes. We observe an ∼5-day delay between the onset of fluid injection and the mainshock, a b-value of 0.78 for the sequence, and a maximum earthquake magnitude larger than the prediction based on the total injection volume, suggesting that the M_w 4.6 sequence occurred on a pre-existing fault and that the maximum magnitude is likely controlled by tectonic conditions. A reprint of this publication is included in Appendix C.

2. Yu, H., R.M. Harrington, H. Kao, Y. Liu, R.E. Abercrombie, and B. Wang (2020). Well proximity governing stress drop variation and seismic attenuation associated with hydraulic fracturing induced earthquakes, *Journal of Geophysical Research: Solid Earth, 125*, e2020JB020103, https://doi.org/10.1029/2020JB020103.

   In this study, we find that earthquakes close to the injection well have lower stress drop values than those at greater distance. Stress drop values are generally invariant within clusters either proximal (~0.1–1 MPa) or distal (~1–10 MPa) to the well, suggesting that dynamic ruptures in rocks with similar rheological properties tend to have relatively constant stress drop values. A reprint of this publication is included in Appendix D.

3. Babaie Mahani, A., S. Venables, H. Kao, R. Visser, M. Gaucher, R.M.H. Dokht, and J. Johnson (2021). Intensity of induced earthquakes in northeast British Columbia, Canada, *Seismological Research Letters, 92*, 3482-3491, https://doi.org/10.1785/0220210037.

   This paper investigates the intensity distribution of induced earthquakes in northeast BC. Although intensities from shallow earthquakes (depth ≤5 km) can be higher than deep events (depth ≥10 km), at close distances (10–15 km), they tend to decrease abruptly at greater distances to become lower than deep events. The localization of large intensities from induced earthquakes within the meizoseismal area warrants special attention in future resource developments and call for systematic intensity data collection in the WCSB. A reprint of this publication is included in Appendix E.

4. Gao, D., H. Kao, and B. Wang (2021). Misconception of waveform similarity in the identification of repeating earthquakes, *Geophysical Research Letters, 48*, e2021GL092815, https://doi.org/10.1029/2021GL092815.

   In this study, we reveal that the cross-correlation coefficient (CC) is not a reliable proxy for repeating earthquakes. For reliable repeater identification, a better alternative is to require the inter-event distance to be smaller than the rupture area of the larger event. A reprint of this publication is included in Appendix F.

5. Yu, H., R.M. Harrington, H. Kao, Y. Liu, and B. Wang (2021). Fluid-injection induced earthquakes characterized by hybrid-frequency waveforms manifest the transition from aseismic to seismic slip, *Nature Communications, 12*, 6862, https://doi.org/10.1038/s41467-021-26961-x.

   In this paper, we report a new type of injection-induced earthquake, named "earthquakes characterized by hybrid-frequency waveforms" (EHW), that are characterized by broader P- and S-pulses and relatively lower-frequency coda content. The slower rupture speed and/or lower stress drop values of EHW probably represent the manifestation of slow rupture transitioning from aseismic to seismic slip. A reprint of this publication is included in Appendix G.

6. Wang, B., A. Verdecchia, H. Kao, R.M. Harrington, Y. Liu, and H. Yu (2021). A study on the largest hydraulic fracturing induced earthquake in Canada: numerical modeling and triggering mechanism, *Bulletin of the Seismological Society of America, 111*, 1392-1404, https://doi.org/10.1785/0120200251.

   This paper focused on the investigation of the triggering mechanism of the largest hydraulic fracturing-induced earthquake in BC (i.e., the 17 August 2015, M_w 4.6, earthquake northwest of Fort St. John). Three finite-element 3D poroelastic models of various permeability structures and presence or absence of hydraulic conduits are constructed to calculate the coupled evolution of elastic stress and pore pressure caused by multistage fluid injections. Our simulation results suggest that pore pressure increase associated with the migration of injected fluid is required to accumulate sufficient stress perturbations to trigger the M_w 4.6 earthquake. A reprint of this publication is included in Appendix H.

7. Gao, D., H. Kao, B. Wang, R. Visser, R. Schultz, and R.M. Harrington (2022). Complex 3D migration and delayed triggering of hydraulic fracturing-induced seismicity: A case study near Fox Creek, Alberta, *Geophysical Research Letters, 49*, e2021GL093979, https://doi.org/10.1029/2021GL093979.

   Earthquakes resulting from hydraulic fracturing (HF) can have delayed triggering relative to injection commencement over a varied range of time scales. In this study, we revisit the famous 2015 Fox Creek HF-induced earthquake sequence with high-resolution earthquake relocation methods. Our results reveal a complex first-outward-then-inward IIE migration pattern. This 3D pattern can successfully explain the observed delayed triggering and required rapid pore-pressure build-up from HF at local distance. A reprint of this publication is included in Appendix I.

WP4: Delineation of Significant Factors that Control the Seismogenesis of IIE

With the outputs from the previous three work plans, this fourth work plan was to establish a susceptibility model for the IIE in northeast BC based on its geological, tectonic, geomechanical, and hydrological conditions to mitigate IIE-related seismic hazard. This work is specifically mentioned and recommended by the BC Scientific Hydraulic Fracturing Review Panel.

Under this work plan, we first investigated the temporal changes in the frequency-magnitude distributions of multiple IIE clusters in regions where the level of background seismicity is low. The calculated seismogenic indices agree very well with the expected seismic response to hydraulic fracturing and wastewater disposal and show a strong correlation with tectonically accumulated strain energy. Second, we explored the relative significance of the potential controlling factors of IIE. The top three influential factors are injection type, regional structural geology, and stratigraphy. We propose a physical model to interpret the observed contrasting seismogenic behaviors of IIE in northeast BC. We also propose a schematic model to interpret our finding as shown in Fig. 6. Third, we applied the XGBoost machine learning algorithm and Shapley Additive exPlanations (SHAP) to delineate and interpret potential controlling factors of IIE in the northern Montney Play. The results show that both geological and operational factors can impact the distribution of IIE with the top four being the horizontal distance between injection and the Cordilleran foreland thrust and fold belt, the cumulative injected volume, shut-in pressure, and the vertical distance to the Debolt formation (Fig. 7).

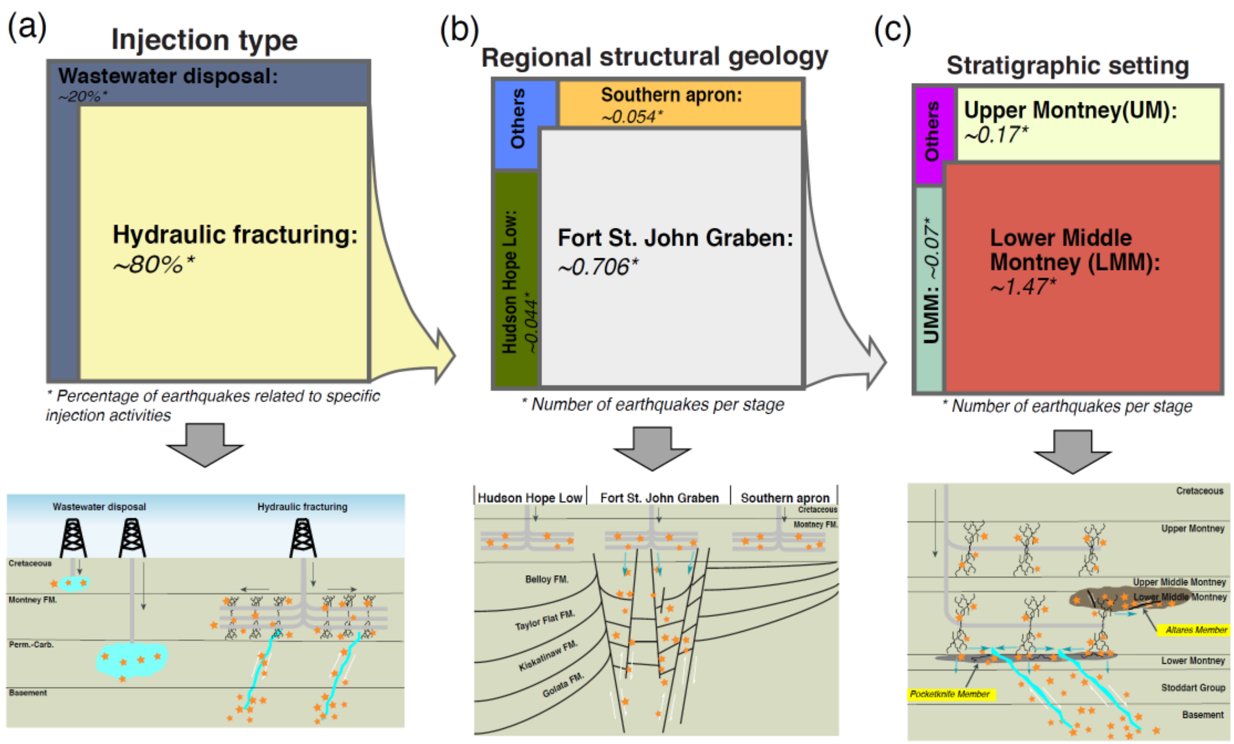

Figure 6. A schematic diagram showing the relative significance of physical factors controlling the

IIE in the southern Montney Play. The bottom sketches illustrate the corresponding seismogenic mechanisms of IIE for the top three factors. (a) Injection type is the most important factor. Approximately 80% of all IIE (orange stars) are related to hydraulic fracturing (HF) and can occur in the vicinity of injection depth and the basement via hydraulic conduits. (b) Regional structural geology is the second most important factor. The number of earthquakes per HF stage is the highest within the Fort St. John Graben filled with subvertical faults. Blue arrows show the potential fluid migration along the graben faults. (c) Stratigraphic setting is the third most important factor. The numbers of earthquakes per HF stage is the highest when the Lower-Middle Montney (LMM) is the HF target. The higher IIE rate may be related to the presence of the Altares Member and Pocketknife Member along the top and bottom sections of the LMM, respectively. Horizontal blue arrows show the fluid migration along the bedding contacts and possibly intersecting with graben faults, while the small vertical blue arrows show the slow diffusion via the permeable Permo-Carboniferous formations below the LMM.

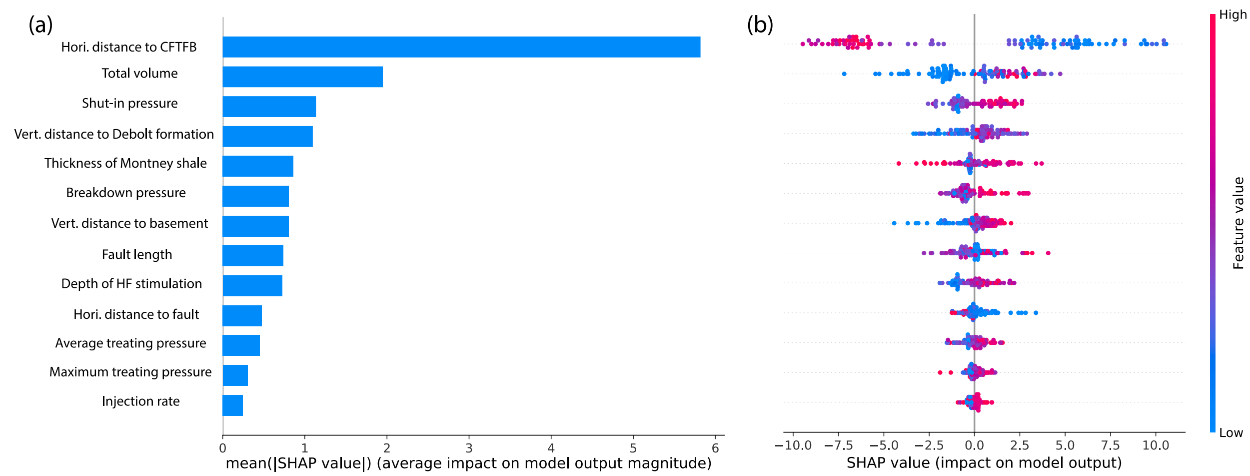

Figure 7. SHAP values of various geological and operational factors. (a) Mean SHAP values of the XGBoost model, representing the relative importance to the model output. The features are ordered based on their importance. (b) Detailed distribution of SHAP values of all cells. Each dot represents one specific feature of a cell and is coloured by the feature's SHAP value. A higher positive SHAP value means this factor would induce more IIE in a cell than the average number of IIE of all cells.

Key outputs are summarized below:

1. Dokht, R.M.H, H. Kao, A. Babaie Mahani, and R. Visser (2021). Spatiotemporal analysis of seismotectonic state of injection-induced seismicity clusters in the Western Canada Sedimentary Basin, *Journal of Geophysical Research: Solid Earth, 126,* e2020JB021362, https://doi.org/10.1029/2020JB021362.

   In this study, we investigate the temporal changes in the frequency-magnitude distributions for multiple clusters of induced events in regions where the level of background seismicity is low. The calculated seismogenic indices agree very well with the expected seismic response to hydraulic fracturing and wastewater disposal and show a strong correlation with tectonically accumulated strain energy. A reprint of this publication is included in Appendix J.

2. Wang, B., H. Kao, H. Yu, R. Visser, and S. Venables (2022). Physical factors controlling the diverse seismogenic behavior of fluid injections in western Canada, *Earth and Planetary Science Letters, 589*, 117555, https://doi.org/10.1016/j.epsl.2022.117555.

   In this paper, we explore the relative significance of the potential controlling factors of IIE. The top three influential factors are injection type, regional structural geology, and stratigraphy. We propose a physical model to interpret the observed contrasting seismogenic behaviors of IIE in northeast BC. A preprint of this publication is included in Appendix K.

3. Wang, B., H. Kao, R.M.H. Dokht, R. Visser, and H. Yu (2022). Delineating the Controlling Factors of Hydraulic Fracturing-Induced Seismicity in the Northern Montney Play using XGBoost Model, *Seismological Research Letters*, https://doi.org/10.1785/0220220075.

   This study applies the XGBoost machine learning algorithm (XGBoost-MLA) to delineate potential controlling factors of IIE in the northern Montney Play. The results show that both geological and operational factors can impact the distribution of IIE with the top four being the horizontal distance between injection and the Cordilleran deformation front, the cumulative injected volume, shut-in pressure, and the vertical distance to the Debolt formation. A preprint of this publication is included in Appendix L.

Conclusions

For this Geoscience BC research project, objectives of the four proposed work plans (WP) were achieved.

For WP1, we ensure the continuing operation of the McGill Array (FDSN network code XL), and worked closely with our partners, including NRCan, BCOGC, and Ruhr University Bochum (RUB), to coordinate maintenance services to seismograph stations in the Montney area (FDSN network codes 1E and PQ). All seismograph stations are transmitting data directly to the Apollo server in NRCan's Sidney office for real-time processing. More significantly, all seismic data are archived in the Data Management Center of the Incorporated Research Institutions for Seismology (DMC, IRIS) for free distribution.

For WP2, we built the most comprehensive and accurate earthquake catalogues for northeast BC, by detecting and locating 23753 earthquakes within the KSMMA during 2019–2021. These catalogues have an impressive magnitude of completeness of ~0.8.

For WP3, we delineated source characteristics not only for the largest IIE, but also for smaller sequences proximal to HF wells in northeast BC and find that the stress drop values of IIE in the study area are within the range of tectonic events, but toward the lower end. We also investigated the possible triggering mechanisms for the largest IIE in the WCSB, and propose that pore pressure increase associated with the migration of injected fluid via high permeable conduits is required to accumulate sufficient stress perturbation to trigger the M_w 4.6 earthquake. Meanwhile, we report a new type of injection-induced earthquakes, named "earthquakes characterized by hybrid-frequency waveforms" (EHW). EHW events generally have broader P- and S-pulses and relatively lower frequency content in the coda wave train. The slower rupture speed and/or lower stress drop values of EHW probably represent the manifestation of slow rupture transitioning from aseismic to seismic slip.

For WP4, we analyzed the contrasting seismogenic behaviors of IIE in northeast BC and delineated the top three influential factors as injection type, regional structural geology, and stratigraphy. Based on the relative importance of the controlling factors, we propose a physical model to interpret the observed seismic pattern. We also established a susceptibility model for the IIE in northeast BC with the XGBoost machine learning algorithm that includes geological, tectonic, geomechanical, and hydrological factors.

The fruitful outcomes of this project improve our understanding of the source process of IIE in northeast BC. Our results also benefit BCOGC and the energy industry by providing insightful models that would lead to more effective mitigation of seismic hazard from IIE.

Finally, we emphasize the importance of high-resolution, long-term monitoring of local seismicity and crustal deformation in areas of active HF and WD. In particular, the physical mechanisms responsible for delayed IIE events (i.e., events that occurred after injection was completed) deserve further investigation as the Traffic Light Protocol for Induced Seismicity currently implemented by BCOGC may not be applicable to such events. Identification of precursory signals and/or reliable proxies of the physical processes leading to the occurrence of significant IIE ruptures can also be an important next step toward establishing a proactive strategy of seismic risk assessment and mitigation. Various types of datasets (geological, geophysical, geomechanical, seismic, etc.) collected by individual operators in northeast BC can potentially offer observational constraints that are unavailable with public networks. Close collaboration and transparent data sharing between the research community and the energy industry should be strongly encouraged and facilitated.

References

1 Porter, J., Price, R. & McCrossan, R. The western Canada sedimentary basin. *Philosophical Transactions of the Royal Society of London. Series A, Mathematical and Physical Sciences* **305(1489)**, 169-192 (1982).

2 BC Oil and Gas Commission. British Columbia's Oil and Gas Reserves and Production Report 2017. 40pp. https://www.bcogc.ca/node/15405 (2019).

3 Farahbod, A. M., Kao, H., Cassidy, J. F. & Walker, D. How did hydraulic fracturing operations in the Horn River Basin change the seismicity patterns in northeast British Columbia, Canada? *The Leading Edge* **34**, 658–660, 662–663, doi:10.1190/tle34060658.1 (2015).

4 Farahbod, A. M., Kao, H., Walker, D. M. & Cassidy, J. F. Investigation of regional seismicity before and after hydraulic fracturing in the Horn River Basin, northeast British Columbia. *Can. J. Earth Sci.* **52**, 112-122, doi:10.1139/cjes-2014-0162 (2015).

5 Atkinson, G. M. *et al.* Hydraulic fracturing and seismicity in the Western Canada Sedimentary Basin. *Seismological Research Letters* **87**, 631-647, doi:10.1785/0220150263 (2016).

6 Babaie Mahani, A. *et al.* Fluid injection and seismic activity in the northern Montney Play, British Columbia, Canada, with special reference to the 17 August 2015 Mw 4.6 induced earthquake. *Bull. Seismol. Soc. Am.* **107**, 542-552, doi:10.1785/0120160175 (2017).

7 Ellsworth, W. L. Injection-induced earthquakes. *Science* **341**, 1225942, doi:10.1126/science.1225942 (2013).

8 Lei, X., Wang, Z. & Su, J. The December 2018 ML 5.7 and January 2019 ML 5.3 Earthquakes in South Sichuan Basin Induced by Shale Gas Hydraulic Fracturing. *Seismological Research Letters*, doi:10.1785/0220190029 (2019).

9 Rubinstein, J. L., Ellsworth, W. L. & Dougherty, S. L. The 2013–2016 Induced Earthquakes in Harper and Sumner Counties, Southern Kansas. *Bulletin of the Seismological Society of America* **108**, 674-689, doi:10.1785/0120170209 (2018).

10 Hough, S. E. & Page, M. A Century of Induced Earthquakes in Oklahoma? *Bulletin of the Seismological Society of America* **105**, 2863-2870, doi:10.1785/0120150109 (2015).

11 Farahbod, A. M., Cassidy, J. F., Kao, H. & Walker, D. Collaborative studies of regional seismicity in northeast British Columbia. *Can. Soc. Explo. Gephys. Recorder* **39**, 40-44 (2014).

12 Kao, H., Eaton, D. W., Atkinson, G. M., Maxwell, S. & Babaie Mahani, A. Technical meeting on the traffic light protocol (TLC) for induced seismicity: Summary and recommendations. *Geol. Surv. Canada Open-File Report* **8075**, 20 pp., doi:10.4095/299002 (2016).

13 Barbaie Mahani, A. *et al.* Ground motion characteristics of the November 30, 2018 injection-induced earthquake sequence in northeastern British Columbia, Canada. *Seismol. Res. Lett.* **90**, 1457-1467, doi:10.1785/0220190040 (2019).

14 Babaie Mahani, A., Kao, H., Johnson, J. & Salas, C. J. Ground motion from the August 17, 2015, moment magnitude 4.6 earthquake induced by hydraulic fracturing in northeastern British Columbia. *Geoscience BC Report* **2017-1**, 9-14 (2017).

15 Visser, R. *et al.* A comprehensive earthquake catalogue for northeastern British Columbia and western Alberta, 2014–2016. *Geol. Surv. Canada Open-File Report* **8335**, 27 pp., doi:10.4095/306292 (2017).

16 Yeck, W. L. *et al.* Far-field pressurization likely caused one of the largest injection induced earthquakes by reactivating a large preexisting basement fault structure. *Geophysical Research Letters* **43**, 10,198-110,207, doi:10.1002/2016GL070861 (2016).

17 Visser, R. *et al.* A comprehensive earthquake catalogue for the Fort St. John–Dawson Creek region, British Columbia, 2017–2018. *Geol. Surv. Canada Open-File Report* **8718**, 30 pp., doi:10.4095/326015 (2020).

18 Zhai, G. & Shirzaei, M. Fluid injection and time-dependent seismic hazard in the Barnett Shale, Texas. *Geophysical Research Letters* **45**, 4743-4753, doi:10.1029/2018GL077696 (2018).

19 Scientific Hydraulic Fracturing Review Panel. Scientific Review of Hydraulic Fracturing in British Columbia. 236pp, https://www232.gov.bc.ca/assets/gov/farming-natural-resources-and-industry/natural-gas-oil/responsible-oil-gas-development/scientific_hydraulic_fracturing_review_panel_final_report.pdf (2019).